



Formation of oleogels based on emulsions stabilized with cellulose nanocrystals and sodium caseinate

Downloaded from: <https://research.chalmers.se>, 2025-12-04 23:22 UTC

Citation for the original published paper (version of record):

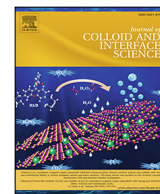
Urbánková, L., Sedlacek, T., Kašpárková, V. et al (2021). Formation of oleogels based on emulsions stabilized with cellulose nanocrystals and sodium caseinate. *Journal of Colloid and Interface Science*, 596: 245-256.
<http://dx.doi.org/10.1016/j.jcis.2021.02.104>

N.B. When citing this work, cite the original published paper.



Contents lists available at ScienceDirect

Journal of Colloid and Interface Science

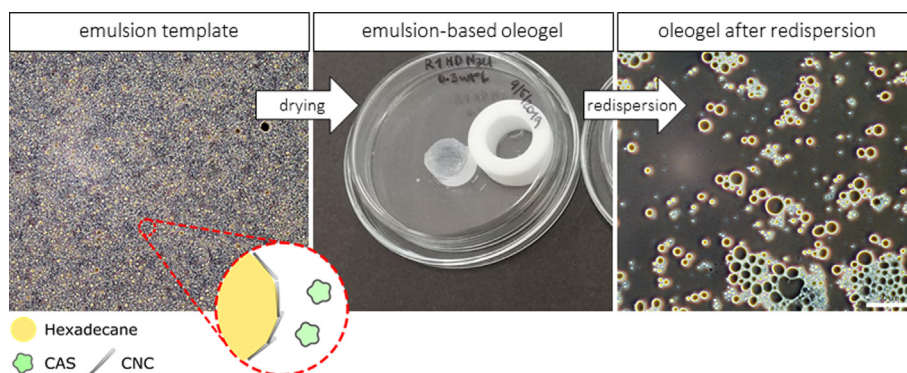
journal homepage: www.elsevier.com/locate/jcis

Regular Article

Formation of oleogels based on emulsions stabilized with cellulose nanocrystals and sodium caseinate

Lucie Urbánková^{a,b}, Tomáš Sedláček^{a,b}, Věra Kašpárková^{a,b}, Romain Bordes^c^a Department of Fat, Surfactant and Cosmetics Technology, Faculty of Technology, Tomas Bata University in Zlín, nám. T. G. Masaryka 5555, 760 01 Zlín, Czech Republic^b Centre of Polymer Systems, Tomas Bata University in Zlín, nám. T. G. Masaryka 5555, 760 01 Zlín, Czech Republic^c Chalmers University of Technology, Department of Chemistry and Chemical Engineering, SE-412 96 Göteborg, Sweden

GRAPHICAL ABSTRACT



ARTICLE INFO

Article history:

Received 11 November 2020

Revised 24 January 2021

Accepted 23 February 2021

Available online 9 March 2021

Keywords:

Emulsion

Cellulose nanocrystals

Sodium caseinate

Oleogel

Viscoelastic properties

Redispersibility

ABSTRACT

Hypothesis: In the preparation of oleogels based on Pickering-emulsions, the choice of the preparation route is critical to withstand drying under ambient conditions, as it conditions the composition of the interfacial layer at the oil-water interface.

Experiments: Hexadecane and olive oil oleogels were prepared using an emulsion-template approach from oil-in-water emulsions formulated with cellulose nanocrystals (CNC) and sodium caseinate (CAS) added in different orders (CNC/CAS together; first CAS then CNC; first CNC then CAS). The oleogels were formed from pre-concentrated emulsions by drying at ambient temperature. The structure of the gels was characterised by confocal laser scanning microscopy, and the gels were assessed in terms of viscoelastic properties and redispersibility.

Findings: The properties of oleogels were controlled by 1) the composition of the surface layer at oil-water interface; 2) the amount and type of non-adsorbed stabilizer; and 3) the composition and viscosity of oils (hexadecane vs. olive oil). For the oleogels prepared from starting emulsions stabilized with CNC with subsequent addition of CAS, and free CAS present in aqueous phase, the elastic component was prevalent. Overall, the dominating species at the oil-water interface controlled the emulsion behaviour and stability, as well as viscoelastic behaviour of the resulting oleogels and their redispersibility.

© 2021 The Authors. Published by Elsevier Inc. This is an open access article under the CC BY license (<http://creativecommons.org/licenses/by/4.0/>).

E-mail addresses: urbankova@utb.cz (L. Urbánková), sedlacek@utb.cz (T. Sedláček), vkasparkova@utb.cz (V. Kašpárková), bordes@chalmers.se (R. Bordes)

<https://doi.org/10.1016/j.jcis.2021.02.104>

0021-9797/© 2021 The Authors. Published by Elsevier Inc.

This is an open access article under the CC BY license (<http://creativecommons.org/licenses/by/4.0/>).

1. Introduction

The development of structured liquid oil-based gels (oleogels) has attracted a great deal of interest from researchers looking for cross-linking agent-free ways to convert liquid oils into gel-like substances [1], often aiming at using liquid oil-based soft solids in drug delivery and food related applications. There are two main physical approaches for preparing oleogels. It can be either a direct oleogelation using a structuring agent in the oil phase [2,3] or an indirect method employing emulsions as templates followed by water removal [1,4–6].

Direct oleogelation can be achieved by using several types of structuring agents, such as phytosterols, fatty acids, waxes, monoacylglycerols or cellulose derivatives [7]. For drug delivery applications, one of the most promising structuring agents is ethylcellulose as it is the only known polymer oleogelator directly dispersible in oil. Ethylcellulose has been successfully used for oleogelation of virgin olive oil [8] in combination with behenic acid [9] or hydroxypropyl methylcellulose [10].

On the other hand, the so-called indirect oleogelation uses oil-in-water emulsion as a template and is realised through complete removal of the water phase. Patel, et al. (2015) studied oleogelation using a hydrophilic matrix of biopolymers. Their method involved oil-in-water emulsion template stabilized by gelatin and xanthan gum [3] with water removal at high and low temperatures. In the study of Alizadeh, et al. (2020), the oil-in-water emulsion templates of sunflower oil/beeswax were stabilized using sodium caseinate, hydroxypropyl methylcellulose or their mixtures [11]. Here the main challenge lies in that the emulsion must be stable enough to withstand water removal. It implies an interfacial composition that can accommodate the stress built during droplets confinement leading to a flattening of the interface. Pickering emulsion lend themselves well for the purpose as the interface stabilization has shown good resistance to stress by allowing the formation of high internal phase emulsion [12].

In the current study we build on the experience gathered in a previously published study [13] where cellulose nanocrystals (CNCs) were employed in combination with sodium caseinate (CAS) to stabilize emulsions. We present an approach to produce oleogel that employs physical trapping of a hydrophobic liquid oil in a matrix prepared using a two-step process. The first step comprises formulating a surfactant-free oil-in-water emulsion stabilized by protein and cellulose nanoparticles, followed in the second step by removal of the water phase by centrifugation and evaporation. This allows the formation of a matrix of water-soluble biopolymer and nanoparticles. Oleogels were formulated with hexadecane and olive oil, of which the latter may find use as a suitable carrier for bioactive lipophilic substances. The principal novelty of this approach lies primarily in using emulsions as template, where a combination of CNC (Pickering stabilizer) and sodium caseinate (surface active) allowed drying at room temperature. The emulsions for preparing oleogels are traditionally stabilized with standard polymers and biopolymers, which work by a different stabilization mechanism, and often partly phase separate during drying. The advantage of the reported system is also the unique ability of CNC and CAS to form oleogels at low stabilizer concentrations and without additional thickeners.

2. Materials and methods

2.1. Materials

Hexadecane and casein sodium salt from bovine milk (CAS) were purchased from Sigma-Aldrich (Germany). Cellulose nanocrystal (CNC) powder obtained *via* the sulphuric acid hydrol-

ysis was purchased from CelluForce (Canada). Extra virgin olive oil was from a local store. Calcium chloride (CaCl_2) and sodium chloride (NaCl), obtained from Sigma Aldrich and Merck (Germany) were of analytical grade. Fluorescein sodium salt (98.5–100.5%) was from Riedel-de Haën (Germany). All studies were conducted using Milli-Q water.

2.1.1. Preparation of emulsions and oleogels

2.1.1.1. Preparation of emulsions. CAS dispersions with concentration of 2 wt% were prepared by dispersing CAS powder in Milli-Q water followed with 4 h stirring at ambient temperature. Aqueous CNC dispersions (2 wt%) were prepared by stirring the powder for 12 h followed by ultrasound treatment with UP400S sonicator (Hielscher, Germany) operating at 60% output during three cycles with a duration of 1 min.

Emulsions with o/w ratio of 20/80 (wt/wt) and total particle content (CAS + CNC) of 0.2 or 0.3 wt% were formulated. The oil was dispersed in aqueous phase and emulsified by sonication (UP400S, Hielscher, Germany) at 60% output. The oil phase consisted of hexadecane (HD) or olive oil (OO). The emulsification was conducted using three different routes R1, R2 and R3 described in details in Pindakova, et al. (2019). In brief, in **Route R1** CNC and CAS aqueous dispersions were mixed in a 1:1 ratio, hexadecane or olive oil (20 wt%) was added to CNC/CAS mixture and the system was sonicated for 1 min. In **Route R2** a primary emulsion (PE-R2) containing 40 wt% oil and stabilized by 0.2 wt% CAS dispersion was prepared by sonication (1 min). CNC dispersion at 0.2 wt% was then added to the emulsion and sonicated for 20 s to get the final emulsion with a content of 20 wt% oil and 0.2 wt% particles. In **Route R3** the order of addition of CAS and CNC was inverted. A primary emulsion containing 40 wt% of oil stabilized by 0.2 wt% CNC (PE-R3) was prepared by sonication (1 min). CAS at 0.2 wt% was then added followed by sonication (20 s) which resulted in a final emulsion containing 20 wt% oil and 0.2 wt% particles in total. Correspondingly, emulsions with a total particle content of 0.3 wt% were prepared.

The emulsion aqueous phase contained either NaCl (5 mM) or CaCl_2 (0.5 mM) as background electrolyte, which facilitated emulsification [14].

2.1.1.2. Preparation of oleogels. After emulsification, each of the samples prepared using the three above-described routes R1, R2 and R3 was centrifuged at 6 000 rpm for 3 min (35 g; Hettich EBA 20, Germany) to separate emulsion droplets from supernatant. The separated upper emulsion layer was then carefully transferred to Teflon cylindrical mold (diameter of 12 mm) placed on Petri dish, and dried for 48 h at ambient temperature to constant mass. Content of residual moisture in dried oleogels was verified using thermogravimetric analysis (TGA), (TGA Q500, TA Instruments, Inc, USA) conducted in the temperature range of 20–400 °C under N_2 atmosphere at heating rate 10 °C/min. The moisture content was lower for all OO gels (max. 0.2%) in comparison with HD gels containing 4–5% water. Hence, the moisture content depended rather on the type of the encapsulated oil than the gel formulation.

2.1.2. Characterization of CNC/CAS-stabilized emulsions

2.1.2.1. Size and distribution of the emulsion droplets. All emulsions were analysed at 25 °C for droplet size and distribution by laser diffraction using a Malvern MasterSizer 3000 (Malvern Instruments Ltd; UK). Emulsion droplets absorbance and refractive index were set to 0.001 and 1.421, respectively. Mean droplet size was reported as volume mean diameter ($D_{(4,3)}$).

2.1.2.2. Microstructure of the emulsion. Emulsion droplets were studied using an Olympus CX41 optical microscope with phase contrast (Ph3) (Olympus Corporation, Japan) equipped with the

Quick PHOTO PRO 2.0 software. Prior to observation, a droplet of emulsion (10 μL) was placed onto a glass microscope slide and observed under 10–100 \times magnification. Glass covers were used.

2.1.2.3. Encapsulation efficiency. The encapsulation efficacy (EE) of emulsions was determined following the method reported by Sabliov, et al. (2015) [15]. The volume fraction of non-encapsulated oil was determined after centrifugation of emulsions conducted at 6 000 rpm for 3 min (Hettich EBA 20, Germany). Non-encapsulated oil was removed by microsyringe, and the volume fraction of the oil was re-calculated to its mass fraction using $\rho_{\text{Hexadecane}} = 0.77 \text{ g}\cdot\text{cm}^{-3}$ and $\rho_{\text{Olive oil}} = 0.9087 \text{ g}\cdot\text{cm}^{-3}$. Encapsulation efficiency (%) (EE) was calculated using Eq. (1), where m_o is mass of the non-encapsulated oil and m_T is initial mass of oil phase in the emulsion.

$$EE(\%) = 100 - \left[\frac{m_o * 100}{m_T} \right] \quad (1)$$

2.1.3. Characterization of the oleogels

2.1.3.1. Released oil during drying. The mass of the separated emulsion layer before drying was weighted and let dry to constant mass for 48 h. The mass of dried gel containing released oil was then determined (m_{G+O}), and finally, the mass of oil released by drying was determined (m_o). From these parameters, the amount of released oil (%) (RO) were calculated using Eq. (2).

$$RO(\%) = \frac{m_o}{m_{G+O}} * 100 \quad (2)$$

2.1.3.2. Microstructure of the oleogels. Oleogel microstructure was visualized using an Olympus Fluoview FV3000 confocal laser microscope (Olympus, Japan). For the imaging, the stock dispersions of CAS or CNC (2 wt%) were diluted by fluorescein solution (100 ppm) to concentration of 0.3 wt%. The stained dispersions were then used to prepare emulsions and oleogel samples according to the procedure given in 2.1.1. A thin slice of oleogel was placed onto a glass microscope slide and observed under 40 \times magnification. The wavelength of the laser excitation was 490 nm. Images were acquired and processed with the Olympus FV31S software.

2.1.3.3. Viscoelastic properties. The characterization of the gels was conducted using a rheometer PHYSICA MCR-502 (Anton Paar, Austria) with parallel plate configuration. The diameter of the samples was 12 mm. To avoid slipping of the samples in the instrument geometry, the plates were adjusted by a thin layer of sandpaper. The linear viscoelastic region was established at 1% strain (γ) value. The storage G' and loss G'' moduli were measured as a function of the angle frequency ranging from 50 to 0.1 s^{-1} at a temperature of 25 $^{\circ}\text{C}$.

2.1.3.4. Redispersion of emulsion from dried gels. The oleogels obtained by drying were weighed into Eppendorf vials to which Milli-Q water was added. Masses of the gel and water were chosen to keep the o/w ratio at 20/80, which corresponds to original emulsions. The samples were vortexed for 30 s and let stand for 42–72 h. The emulsions were then visually assessed to determine whether or not the sample re-dispersed to emulsion droplets. Successfully reconstituted samples were observed by optical microscopy on CX41 optical microscope (Olympus Corporation, Japan) with 10–100 \times magnification with the same procedure as described in part 2.2.2.

3. Results and discussion

3.1. Initial o/w emulsions – Comparison of the systems with hexadecane and olive oil

The ability of CAS and CNC particles alone to stabilize hexadecane-water and olive oil-water emulsions was tested and compared before studying the performance of CAS/CNC mixtures under emulsification. For this purpose, primary emulsions containing HD or OO stabilized solely with CAS or CNC particles were prepared and their droplet size distributions were determined (Fig. S1, CAS or CNC). In the case of HD primary emulsions with CAS (PE-R2), the distributions differed from all other curves as they were broader and more flattened. All distributions were multimodal, which also applies to primary emulsions prepared with OO at both concentrations of stabilizers (0.2 and 0.3%). The OO emulsions with CAS displayed a similar course of distributions and differed only in the droplet sizes, which depended on the CAS content. The higher amount of CAS formed smaller droplets, whereas 0.2 wt% CAS yielded droplets with bigger diameter. This difference was due to a lower encapsulation efficacy of 0.2 than 0.3 wt% CAS. At 0.2% CAS content, also a bigger amount of oil remained non-encapsulated (as later verified by encapsulation index EE). Generally, the CAS-stabilized OO emulsions provided droplets with larger sizes than emulsions containing HD.

Contrary to CAS emulsions, the behaviour of the samples stabilized by 0.2 and 0.3 wt% of CNC (PE-R3) was almost identical with the droplet size in similar ranges and absence of free oil. The minor differences among $D_{(3,4)}$ of emulsions with different CNC concentrations resulted from the good emulsification capacity of the CNC particles observed even at such low concentrations.

In the next step, emulsions from mixtures of CAS and CNC added in different order were formulated, and their size ($D_{(4,3)}$) and distribution curves evaluated. As the mechanism of emulsion stabilization with CNC and CAS added in different order was previously described [13], the current study mainly focused on comparison of OO and HD emulsions in terms of their impact on the properties of the oleogels prepared thereof. Moreover, OO used here is more suitable for practical application as it can serve not only as a nutraceutical, but also as a carrier of various lipophilic active substances. Indeed, the main difference in $D_{(4,3)}$ values was observed between emulsions containing different oils (HD or OO), although within each group differences in $D_{(4,3)}$ could be observed originating from the different routes of preparation, stabilizer content and types of electrolyte (Tab. S1). Irrespective of the preparation route, the droplet sizes of HD and OO emulsions ranged from 2.4 to 16.9 μm and 3.6 to 35.8 μm , respectively. The values show that OO formed larger droplets than HD, which is also confirmed by the comparison of the distribution curves of emulsions prepared with 0.3 wt% stabilizers and NaCl (Fig. 1a). The discussed differences likely originate from different character of the used oil phases, which differ in physicochemical properties, such as viscosity, and polarity. For example, the viscosity of the oil can be mentioned; while OO is natural vegetable oil with a relatively high viscosity (84 mPa.s), HD is a hydrocarbon with a viscosity of only 3.4 mPa.s, which probably affects the droplet size extensively. The effect of the dispersed phase viscosity on the droplet size was for example mentioned by Wooster, et al. (2008) who proved that high-viscosity oil phases formed emulsions with larger droplets than oils with low viscosity [16]. This is also in agreement with our observations.

The second parameter, which significantly influenced the droplet size, was the total concentration of stabilizers. Two concentrations (0.2 and 0.3 wt%) were chosen to investigate the effect of this parameter on the droplet size, and subsequently on the structure of

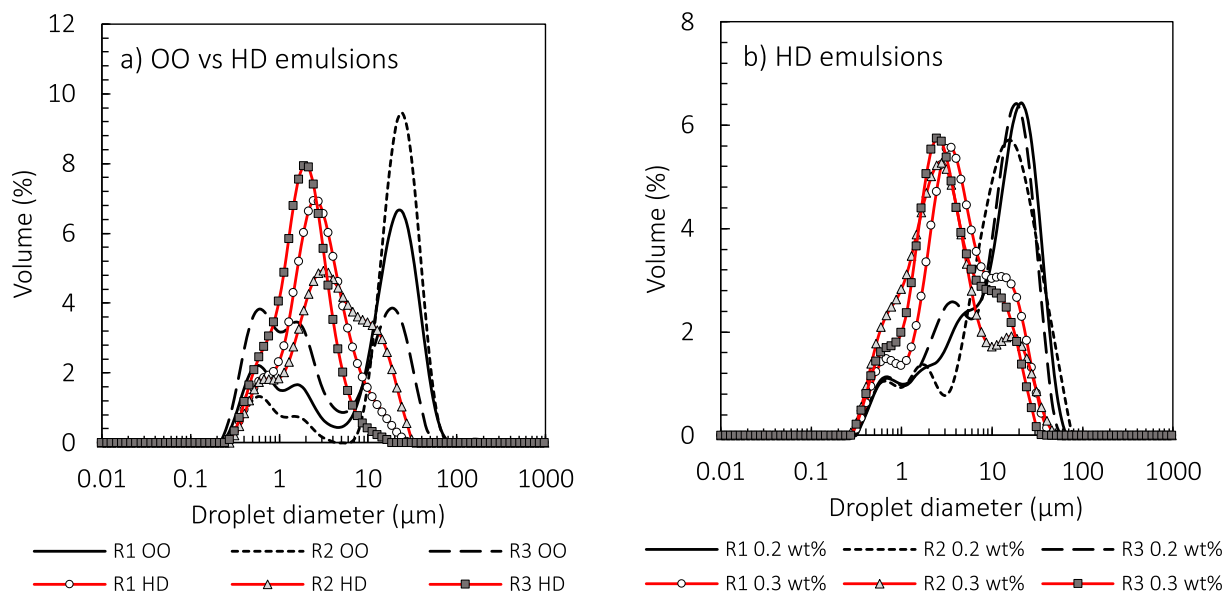


Fig. 1. a) Comparison of the distributions for emulsions with olive oil (OO) and hexadecane (HD) (0.3 wt%, NaCl) prepared via three different routes of CAS and CNC addition (R1, R2, R3); b) Difference between distributions of HD-emulsions prepared with 0.2 and 0.3 wt% stabilizer, in presence CaCl₂. Three different routes of CAS and CNC addition (R1, R2 and R3) are also used.

oleogels. As expected, the emulsions formulated with total higher amount of stabilizers (0.3 wt%) formed smaller droplets than samples prepared with 0.2 wt% of CNC/CAS due to higher amount of stabilizer available to cover the higher surface area of smaller droplets (Fig. 1b) [17]. This observation is valid for both oils. The sizing measurements were confirmed with optical microscopy (Fig. S2).

The last parameter playing a role in the emulsion preparation was the order of CAS and CNC addition, and the type of background electrolyte. These parameters were studied to understand the correlations among emulsion droplet size, structure and arrangement of the oil-water interface, and composition of the inter-droplet space with regard to the properties of the final oleogels. These findings complement the knowledge gathered during our previous study [13].

When emulsification routes were compared it was again observed that the emulsions with HD and OO differed with respect to $D_{(4,3)}$. For route R1, where CAS/CNC mixture was used for stabilization, CNC and CAS competed for space at the oil-water interface. It is however likely that CAS dominated thanks to its higher surface activity [18]. The hypothesis of the competitive adsorption of CAS and CNC is probable as at the pH of emulsions which was around 7 there is no attractive interaction between CNC and CAS; both are negatively charged. With regard to HD-emulsions (Fig. S3), the smallest droplets were formulated with a total stabilizer concentration of 0.3 wt% and NaCl as a background electrolyte ($D_{(4,3)}$ 3.8 ± 0.1 μm). Emulsions with OO followed similar trend, however, their droplets were bigger due to the impact of oil properties, as discussed above.

The influence of the preparation route together with the effect of particle/protein concentration and background salt is also evident from microscopy images of emulsions (see Fig. 2 R1-HD). It can be observed that emulsion with 0.3 wt% of CNC/CAS (NaCl) contained smaller droplets, which is in correlation with distribution curves from diffraction measurements showed in Fig. S3. Emulsions prepared by route R1 proved that the samples with CaCl₂ were more flocculated than these containing NaCl, and droplets stabilized by 0.2 wt% of CNC/CAS were larger than these prepared with higher 0.3 wt% CNC/CAS. The summary of droplet sizes expressed as $D_{(4,3)}$ is given in supporting materials (Tab. S1).

Initial stabilization of the oil with CAS followed by the addition of cellulose nanocrystals was used in route R2. Differences in HD and OO emulsions can already be seen on primary CAS emulsions before CNC addition and are also visible after CNC was added. For HD-emulsions, the influence of total stabilizer content on distributions seemed to prevail, as the curves recorded for 0.3 wt% stabilizer and NaCl or CaCl₂ were similar and shifted towards smaller droplet sizes in comparison with the corresponding samples containing 0.2 wt% stabilizer (Fig. 3). It is also noted that free CAS aggregates can be found in solution. The type of electrolyte had only marginal effect.

On the contrary, emulsions with OO appeared to be more affected by the type of electrolyte. In presence of CaCl₂, both emulsions with concentration in stabilizer of 0.2 and 0.3 wt% yielded distributions with similarly positioned main peak and differed only in the content of flocks (Fig. 3), visible as small peaks at higher droplet size. The influence of stabilizer concentration was also observed with optical microscopy (Fig. S4). The observed effect is likely caused by the enhancement of the emulsification efficacy of CNC in presence of CaCl₂, as reported by Mikulcova, et al. (2016), which is evidenced by a shift of the distribution towards a lower droplet size [19].

From the distribution curves of the emulsions prepared by route R2, it is obvious that the droplets after first emulsification with CAS were stabilized solely by the protein, and the subsequent addition of CNC further improved coverage of their interfaces and stability of the emulsion. It can also be speculated that CNC particles stabilized larger emulsion droplets formed from the remaining free oil.

The route R3, where the primary emulsions were stabilized by CNC and to which CAS was added in a second emulsification step, showed the best emulsifying results with the absence of free oil; this was actually observed already for the CNC primary emulsions. In HD-emulsions, the addition of CAS to CNC stabilized droplets slightly decreased their size (Fig. 4) for all formulations except for emulsion containing 0.2 wt% stabilizer and CaCl₂. This indicates that the lower stabilizer content is not capable to compensate for the influence of CaCl₂ electrolyte and agglomerates formed, which is noticeable in Fig. 5.

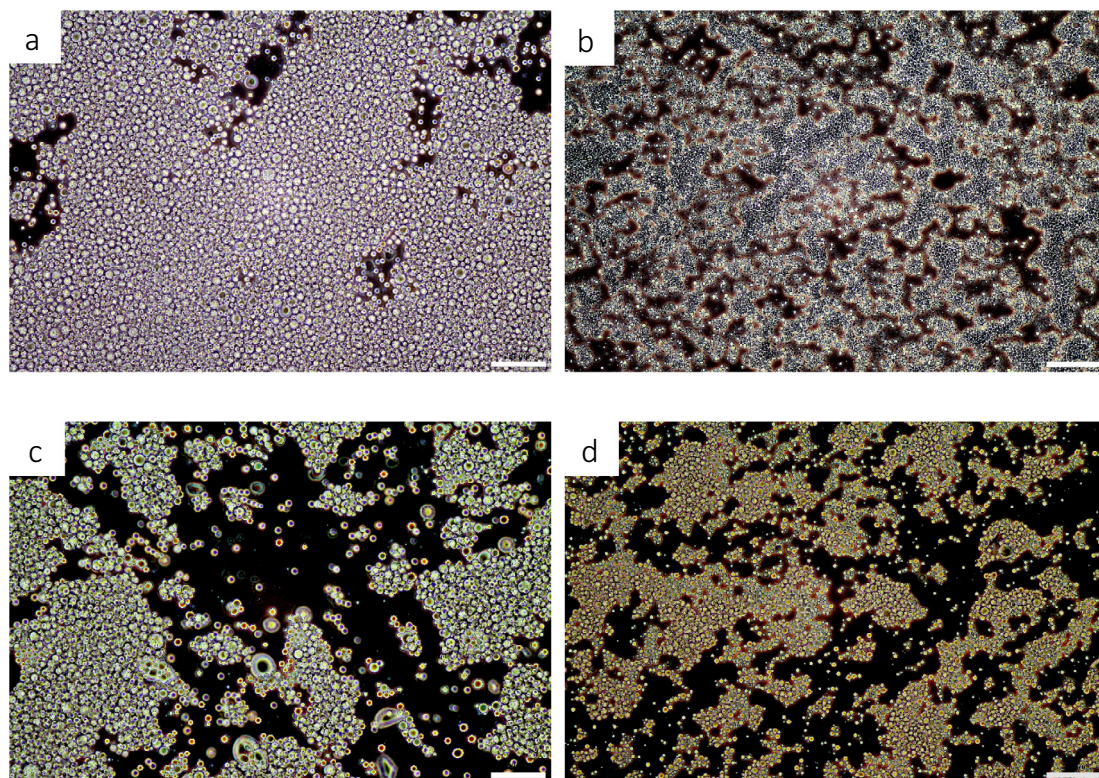


Fig. 2. Microscopy images of HD-emulsions prepared via R1: a) 0.2 wt% NaCl 5 mM; b) 0.3 wt% NaCl 5 mM; c) 0.2 wt% CaCl₂ 0.5 mM; d) 0.3 wt% CaCl₂ 0.5 mM; scale bar is 50 μm.

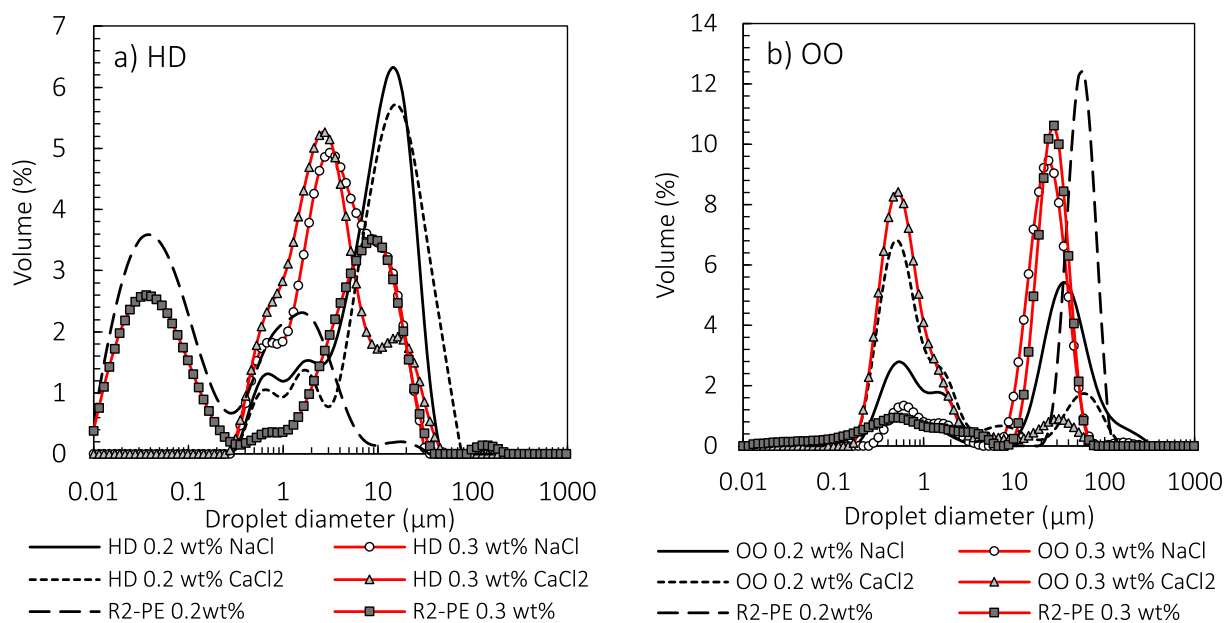


Fig. 3. Distribution curves of studied a) HD-emulsions and b) OO-emulsions prepared by route R2 (primary emulsion stabilized by CAS, subsequent addition of CNC to the aqueous phase). HD stands for hexadecane and OO for olive oil.

The presence of CaCl₂ during emulsification of HD led to an increase in droplet size and their flocculation caused by interaction of the divalent cation with CAS in aqueous phase (Fig. 5a). On the other hand, the synergy between CNC and CAS can be observed for the emulsions with 0.3 wt% stabilizer in presence of NaCl, resulting in monomodal emulsion size distribution (Fig. 5b).

The introduction of CAS to OO emulsions primarily stabilized by CNC shifted the distributions to higher droplet sizes (Fig. 4b). Emulsions prepared via route R3 exhibited multimodal distribution with larger droplets for those containing 0.2% stabilizer, with similar profiles for samples with NaCl and CaCl₂. The microscopy pictures (Fig. S5) illustrate the influence of the electrolyte type on the

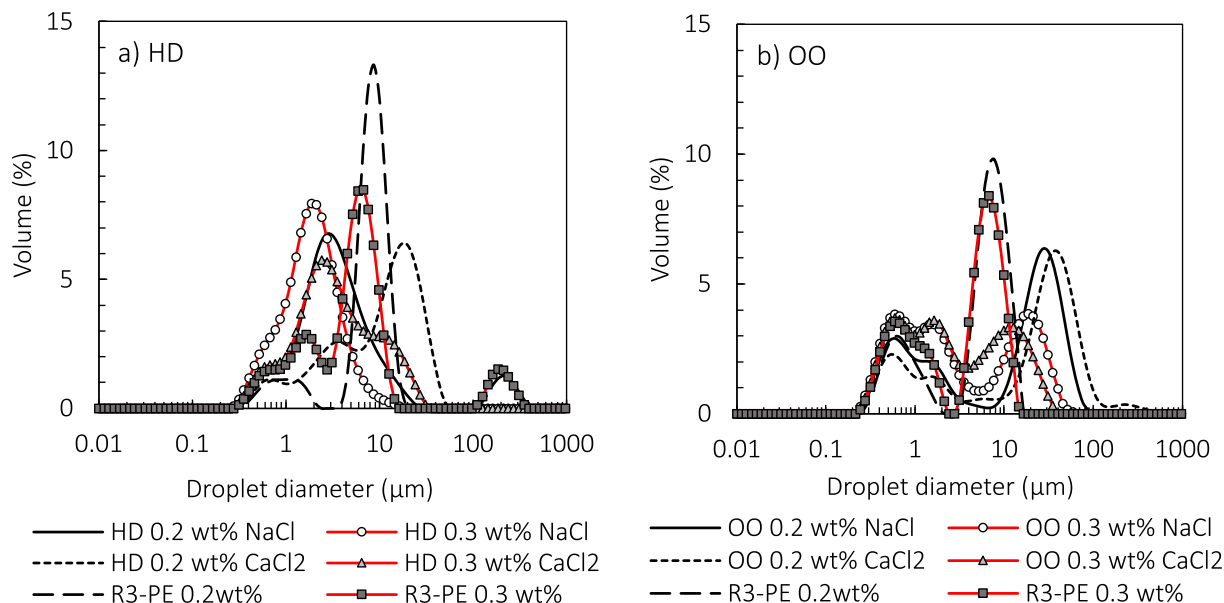


Fig. 4. Distribution curves of studied emulsions prepared by route R3 (primary emulsion stabilized by CNC, subsequent addition of CAS to the aqueous phase).

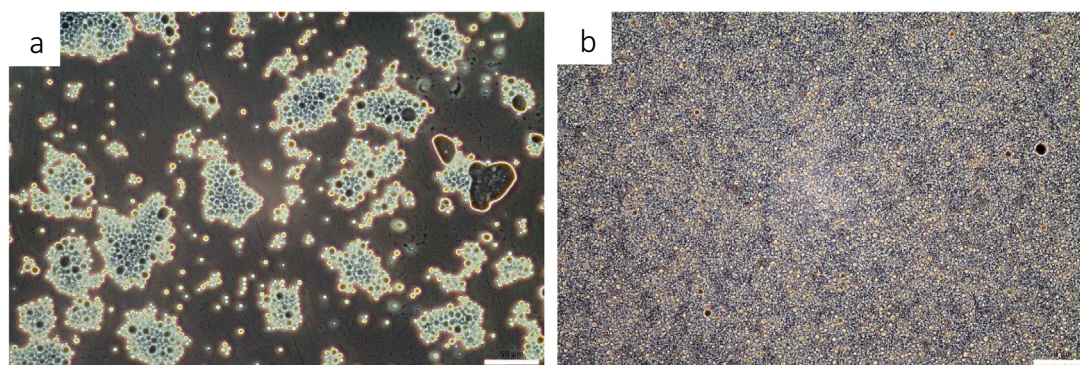


Fig. 5. Microscopy images of HD-emulsions prepared via R3: a) 0.2 wt% CaCl_2 0.5 mM; b) 0.3 wt% NaCl 5 mM; scale bar is 50 μm .

droplet size of the emulsions stabilized with 0.3 wt% stabilizer content.

The stabilization of emulsions prepared by route R3 was likely driven by a strong adsorption of CNC at the oil-water interface followed by the introduction of the more surface active CAS molecules which helped increasing the droplet curvature [13].

3.1.1. Encapsulation efficacy

Although OO-emulsions contained larger droplets and their behaviour was more complicated, encapsulation of the oil was, in comparison with HD emulsions, surprisingly better (Fig. S6). It is seen from the emulsifying efficacy index (%; EE) that reached 100% for all OO containing formulations. The only exception here was the emulsion prepared via route R2 with 0.2 wt% stabilizers and CaCl_2 (EE = 95%). For HD emulsions, the EE was slightly lower and was more affected by the route of preparation, concentration of stabilizing agent and type of background salt (NaCl vs. CaCl_2). Emulsions prepared via route 3 showed the highest EE (98–100%), followed by emulsions from route R1 with EE varying from 85 to 96%. The least efficient formulations displaying a larger variability were the ones prepared by R2 with values from 72 to 100%, 72% being obtained for emulsions prepared by route R2 with 0.2 wt% stabilizers and CaCl_2 . This is likely ascribed to a too low CAS concentration used for formation of primary emulsions leading to non-

encapsulated oil, and also by the effect of CaCl_2 that induced notable CAS aggregation (Ye and Singh 2001; Pind'áková, et al. 2019).

3.2. Emulsion-based gels

The emulsions stabilized only by CNC or CAS did not yield oleogels and only the use of both CAS and CNC allowed drying of the emulsion. Examples of the dried HD oleogels in Fig. 6 show transparent, solid, and compact samples. Oleogels prepared from emulsions containing OO were also transparent but yellowish, owing to the natural colour of olive oil, and their structures were less compact and solid than that of HD-oleogels. The difference originates from the different properties of the oils used, varying droplet sizes of emulsions, as well as from the structure of stabilizing layer at oil-water interface and stabilizers present at inter-droplet space. Furthermore, it is important to note that the drying was always preceded by a centrifugation step that allowed concentrating the emulsion without major oil leakage.

3.2.1. Microstructure of oleogels

The oleogels were observed as structured materials with individual oil droplets separated by a network of stabilizing materials (CAS, CNC) using confocal laser scanning microscopy (CLSM). The water phase was stained with fluorescein. The HD-oleogels

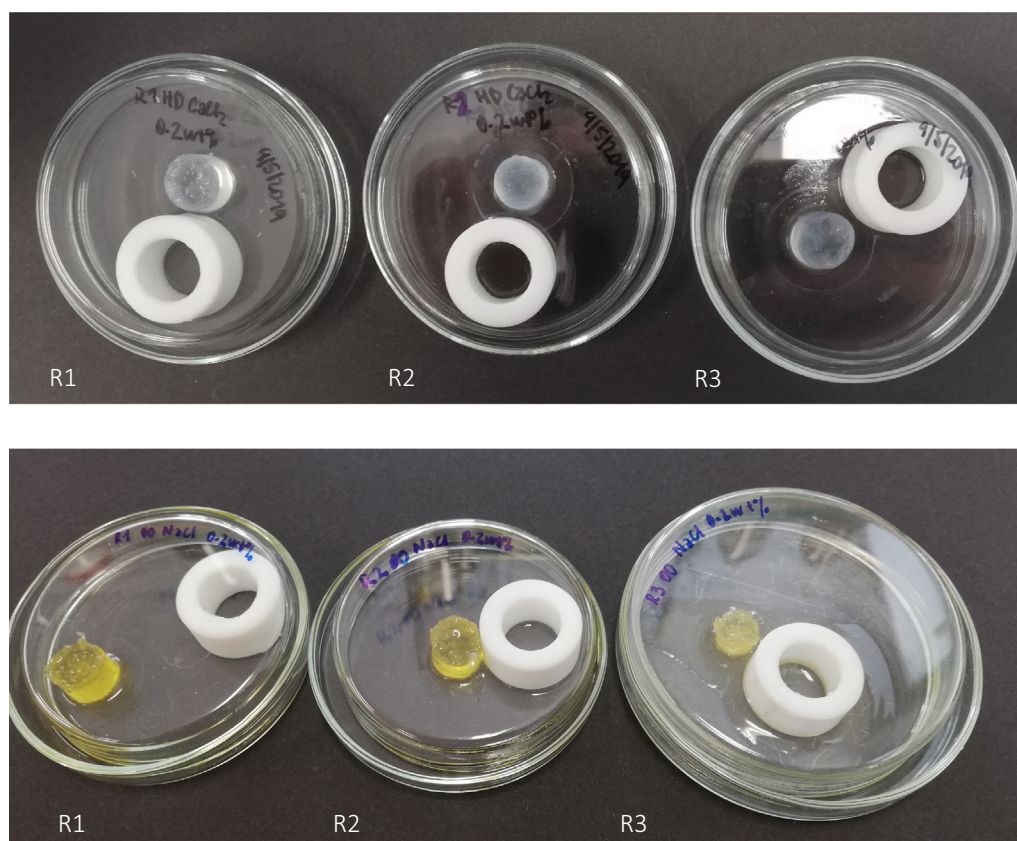


Fig. 6. Dried oleogels prepared from a) hexadecane with 0.2 wt% stabilizer and CaCl_2 0.5 mM and b) olive oil with 0.2 wt% stabilizer and 5 mM NaCl.

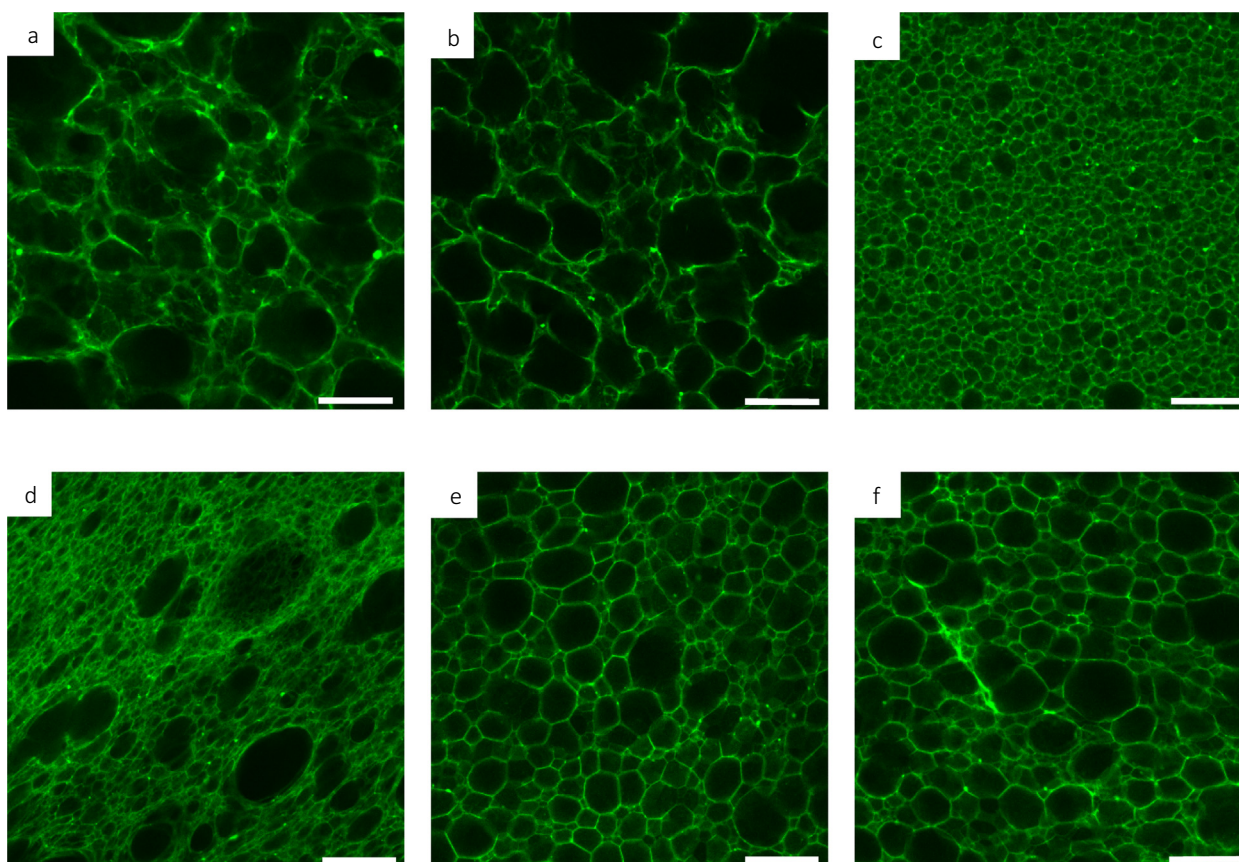


Fig. 7. Microstructure images of hexadecane oleogels a) R1, b) R2, c) R3 and olive oil oleogels d) R1, e) R2, f) R3 (both 0.3 wt%; 5 mM NaCl); scale bar is 30 μm .

prepared via routes R1 and R2 (Fig. 7 a, b) contained larger oil droplets of irregular shape; well defined boundaries between the oil droplets were lost in some of the displayed areas. This can indicate possible coalescence taking place during the drying process. The structure of these oleogels was more heterogeneous, though the gel from the R1 route showed more a thicker polymer matrix around the droplets in comparison with R2 gel. On the contrary, the R3 oleogel (Fig. 7c) was well-structured and more homogeneous. CLSM revealed a tighter arrangement of uniform and smaller droplets, with stronger network of stabilizing agent resulting in oleogel with greater structural stability.

The OO-oleogels prepared via R1 (Fig. 7d) presented dense, mesh-like network of CNC/CAS with embedded oil droplets of smaller size. The structure of oleogel was homogeneous with tightly packed emulsion droplets. The R2 and R3 oleogels (Fig. 7 e, f) showed oil droplets of irregular form and greater sizes. The arrangement of droplets was less dense, with a more open structure.

3.2.2. Release of oil under drying

During water removal, all formulations retained nicely their shape and were stable; nevertheless, a fraction of oil was released. The amount of oil released from the samples is given in Fig. 8. Again, the difference between oleogels containing HD and OO is clear. The amount of oil leaked during drying was in the range of 4–64 % and 17–39% for HD and OO gels, respectively. Here, a closer correlation between the amount of oil released from HD oleogels and the route of their preparation can be seen. For HD-based oleogels, the lowest amount of released oil was for emulsion prepared using route R3, which conforms well to the performance of starting emulsions in terms of droplet size. Emulsion with the smallest droplets (2.4 μm) and lowest oil release (4%) was prepared with the route R3, 0.3 wt% stabilizers and NaCl. For OO-based oleogels, the variability among the preparation routes is, with respect to oil liberation, smaller. Surprisingly, the OO samples prepared via route R2 released a minimal amount of oil. On the other hand, route R2 did not yield emulsion of HD that could be dried without large oil release.

These results underscore the joint effects of two main properties of the parent emulsion during the drying, namely the nature of the oil and the route of preparation. With HD, the presence of CNC during the emulsification was largely beneficial and reduced the oil release. For olive oil, the opposite was observed and it was for the cases where CAS was dominant that the oil release

was at minimum. Even though a general trend relating the oil release with the original droplet size can be put forward, the final details of the resistance to drying depends strongly on the interfacial coverage and nature of the free species in aqueous phase.

3.2.3. Viscoelastic properties of the oleogels

The viscoelastic properties of the oleogels were measured, and the storage (G') and loss (G'') moduli, as well as loss factor ($\tan(\delta)$) were determined. The G' is a measure of the elastic response, whereas G'' corresponds to the viscous response of the material; the loss factor is then the ratio of loss to the storage modulus calculated as $\tan(\delta) = G''/G'$. In case $\tan(\delta) > 1$, the viscous component prevails [20].

In addition to the above-mentioned parameters, the oleogels were characterized by visual observation and during measurements when shear stress was applied to the samples, no leakage of oil was observed. Considering the parameters that influence the viscoelastic behaviour of oleogels, the total concentration of CNC/CAS applied, and the increase of total stabilizer amount from 0.2 to 0.3 wt% raised the gel strength, as indicated by an increase in the storage modulus G' . As an example, the G' of HD-oleogels prepared with the route R1 in presence of NaCl can be mentioned; at angular frequency 0.1 s^{-1} , the storage moduli were 4500 and 16,500 Pa for 0.2 and 0.3 wt% CNC/CAS, respectively. Similar findings were reported by Jiang, et al. (2018), who observed that an increase in the concentration of regenerated cellulose in emulsions stabilized with carboxymethyl cellulose caused an increase in G' resulting in a high gel strength of $G' > 15,000 \text{ Pa}$ [1]. Also, Alizadeh et al. (2020) concluded that concentration of hydroxypropyl methylcellulose and sodium caseinate used to stabilize emulsion were the factors with the most important influence on the textural and rheological properties of the oleogels [11]. Patel, et al. (2015) prepared oleogels by freeze-drying of emulsion stabilized by xanthan gum and gelatine; here the protein–polysaccharide interactions at the oil–water interfaces were exploited to transform liquid oil into oleogels with the strong gel strength ($G' > 11,000 \text{ Pa}$) [3]. The use of two polysaccharides, methylcellulose and hydroxypropyl methylcellulose for oleogel production via emulsion template resulted in hard samples with high mechanical strength. The highest G' of 570,630 Pa was recorded for gels containing 2% methylcellulose and all oleogels here produced showed higher viscoelasticity in comparison with oleogels composed of cellulose ethers mixed with additional components, such as xanthan gum [21].

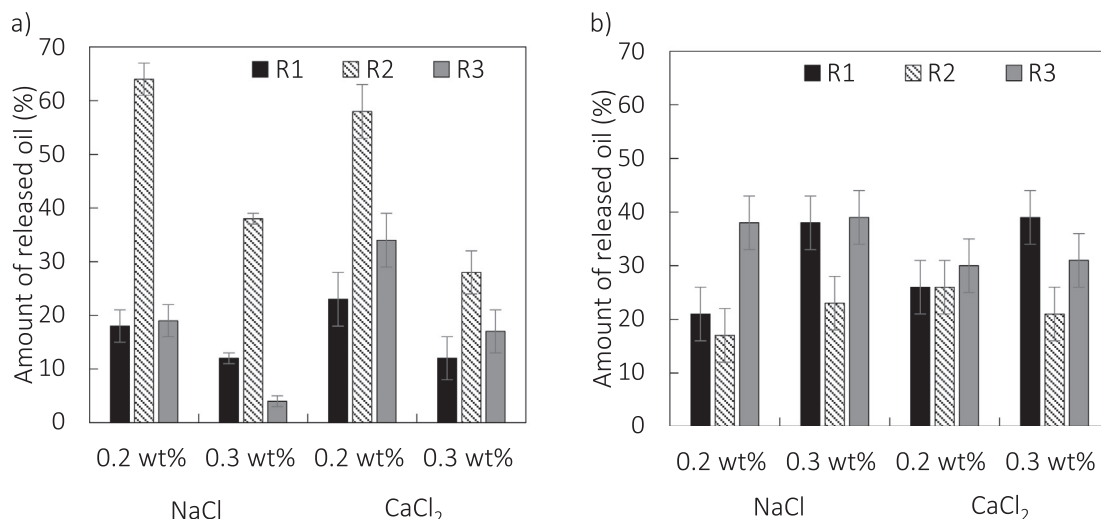


Fig. 8. Amount of oil released during drying of oleogels prepared with emulsifications routes R1, R2, R3 containing a) hexadecane b) olive oil.

For HD-based oleogels with 0.2 wt% of CNC/CAS and NaCl as background salt, the difference among the samples prepared with different routes were also noticeable and G' decreased in the following order: $\bar{G} R3 > \bar{G} R1 > \bar{G} R2$ (Fig. 9). However, when using the 0.3 wt% concentration of CNC/CAS, the observation was different. The values of G' for oleogels prepared by routes R1 and R3 reached almost similar values and were both higher than G' for samples from the route R2. This indicated a higher contribution of the elastic component for oleogels prepared via routes R1 and R3. Another interesting observation for HD-oleogels was the slight dependence of storage modulus on frequency, as the G' with raising angular frequency increased. If we should generalize these results, the HD-oleogels originating from R3-emulsions showed higher elasticity than oleogels prepared via route R1 and R2, with only one exception for HD-oleogels prepared with 0.2 wt% of CNC/CAS and CaCl_2 .

The effect of CNC/CAS concentration on G' values recorded for OO-based oleogels (Fig. 10) correlates to some extent with the

results recorded for samples with HD. The trends of the G' vs frequency dependencies for gels prepared by route R3 were also similar and values of G' were higher than those recorded for oleogels formulated using R2 and R1 routes. This again indicated higher elasticity for this formulation. At the same time, the OO gels from route R1 provided better elasticity than R2 gels, except for formulation from route R1 with 0.3 wt% CNC/CAS and CaCl_2 . This outlying behaviour may be due to the different properties of the starting emulsions in terms of droplet sizes. Emulsions prepared via routes R2 and R3 provided namely significantly smaller droplets (3.6 μm and 6.3 μm , resp.) than the emulsion prepared by the route R1 with the droplet size of 24.7 μm . The higher elastic portion of R2 and R3 oleogels can be, in this particular case, caused by different microstructure of the oleogels. Interestingly, the loss modulus (G'') did not change with increasing frequency, which is indicated by the course of $\tan(\delta)$ showing no significant variations (Fig. 10). This can also indicate that the oil was better encapsulated in this case and did not leak during shearing. In some cases, the

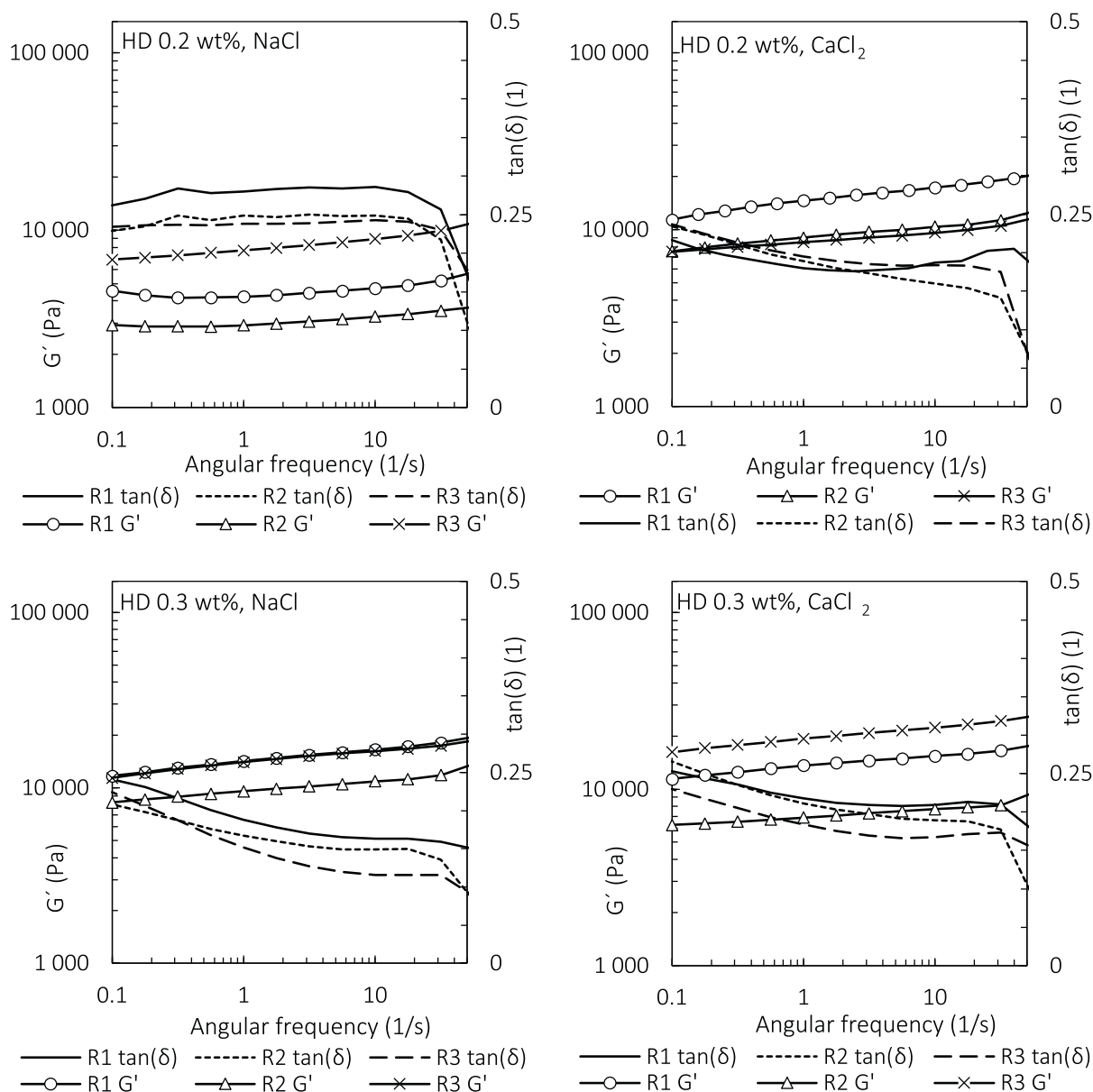


Fig. 9. Dynamic storage moduli (G') and loss factor ($\tan(\delta)$) responses of oleogels prepared from hexadecane emulsions.

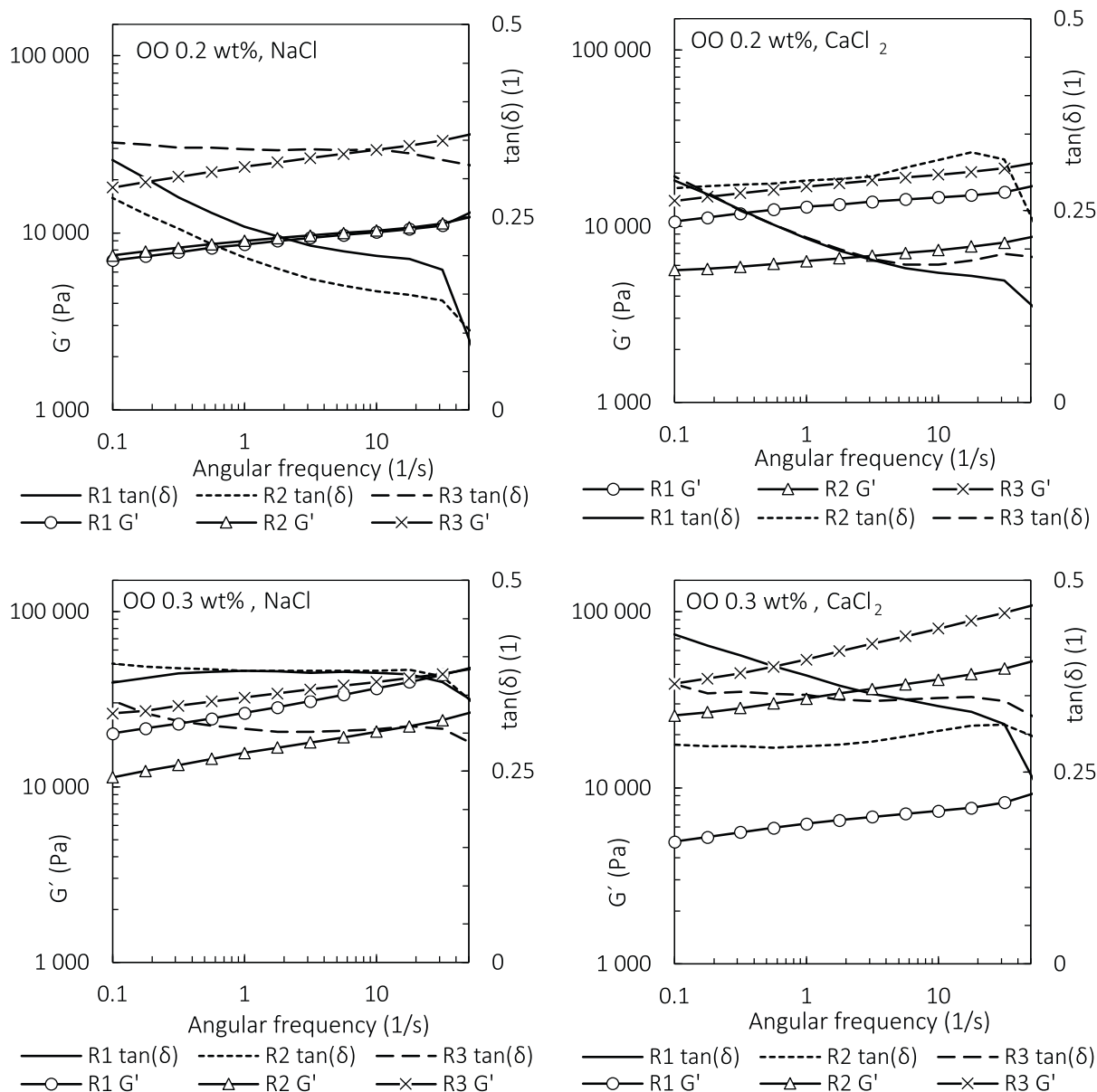


Fig. 10. Dynamic storage moduli (G') and loss factor ($\tan(\delta)$) responses of oleogels prepared from olive oil emulsions.

sharp drop of $\tan(\delta)$ at the highest frequencies was observed showing lower strength of the gel structure for samples prepared by route R1.

Steady state course and values of G'' lower than G' (steady $\tan(\delta)$) over the entire frequency range used are typical for strong gels [22]. Nevertheless, the sharp fall of $\tan(\delta)$ for some formulations at high frequencies may indicate that these oleogels may undergo to a gel to sol transformation.

Taking into account known properties of emulsions used for oleogel formation and their microstructure (Fig. 7), the viscoelasticity is influenced by a combination of various factors, including the droplet sizes in the starting emulsions, the type of background salt and by the route of emulsion preparation. Our findings support the hypothesis that the differences in the arrangements of CNC and CAS at the oil-water interface of the starting emulsions, and the composition of the inter-droplet space described in the previous work [13] play a major role on the ability of emulsions to withstand drying during oleogel formation and subsequently influence their rheological properties. In other words, the nature of the inter-

facial stabilizing layers, i.e. the route of preparation, significantly affected the microstructure of oleogels and controlled their viscoelastic properties.

Protein (sodium caseinate) to polysaccharide (alginate) ratio, together with pH, influenced structural properties of emulsions and oleogels prepared thereof in [23]. Oleogels showed a 10–22 fold G' increase compared to emulsions thanks to the formation of a compact protein-polysaccharide network with tightly packed oil droplets. Also complexes of soy protein isolate and kappa-carrageenan efficiently stabilized emulsions used for preparing oleogels. It was shown that the accumulation of complexes at the interface was responsible for the excellent stability and high gel strength ($G' > 40,000$ Pa) of the gels [24].

In current work, the size of emulsion droplets controlled by the route of emulsification and concentration of CNC/CAS enabled their tighter arrangement during drying, giving rise to a more compact structure. This is supported by the microstructure of HD-oleogels from route R3 (Fig. 7c). Therefore, the elastic portion of modulus prevailed. On the other hand, bigger droplets are packed loosely

with continuous phase filled with free stabilizers and aggregates of CAS (in case CaCl_2 is present), which led to the higher viscosity of the gels.

The type of stabilizing particles dispersed in aqueous phase of emulsions is another factor which influences the viscoelastic properties of the oleogels, and acts in synergy with the droplet size. For the oleogels prepared from emulsions stabilized by the mixture of CNC and CAS (route R1), both CNC and CAS are present between the droplets after the drying of emulsions, as it was reported in our previous work [13]. The oleogel elasticity is therefore influenced by the presence of both CNC and CAS, of which CAS molecules are globular and relatively flexible contrary to the more rigid cellulose nanocrystals. In oleogels prepared via route R2, a fraction of oil remained free after primary emulsification with CAS. However, a portion of the droplets was stabilized later, after CNC was added. Simultaneously, a portion of CNC remained free between the droplets after this second emulsification. This resulted in an emulsion with a mixture of droplets stabilized by both CAS and CNC with CNC dominating in aqueous phase [13]. As CAS is a more flexible molecule and its anchoring at the droplet surface is not as strong for CNC, the final packing of droplets into structure of gel was looser and the oleogel less elastic with more dominant viscous contribution.

For the samples prepared via route R3, the situation was, however, opposite. After the primary emulsification with CNC, almost no oil remained free and the droplets were stabilized by cellulose nanocrystals strongly attached at the oil-water interface. The subsequent addition of flexible CAS with random coil character, induced an even stronger attachment and better deposition of CNC at the oil-water interface, with free CAS molecules forming the matrix between the droplets. The presence of flexible molecules of CAS in the inter-droplets space could therefore contribute to the high elastic modulus of these oleogels.

3.2.4. Redispersion of oleogels

The proof that the emulsion droplets preserved their integrity during drying could be done by testing the redispersion of the oleogels in water. The HD-based oleogels were successfully redispersed, as it is shown by optical microscopy (Fig. S7). The size of the droplet was, however, changed, leaning towards larger size. Moreover, the redispersion of the gels was strongly dependent of the preparation route, and gels prepared from route R2 were the least dispersible. The type of background salt contributed also to differences in gel redispersion, as CaCl_2 induced the formation of insoluble CAS aggregates. The OO-oleogels were not possible to redisperse. A tentative explanation can be based on that the water content of HD-oleogel was significantly higher than that of OO-oleogels, thus offering a more hydrated network that facilitated water penetration upon redispersion.

4. Conclusion

The study reports on the preparation of hexadecane and olive oil oleogels with the aid of an emulsion-template approach. Starting emulsions used for the gel production were stabilized with a combination of cellulose nanocrystals (CNC) working as a Pickering stabilizer and a surface active protein sodium caseinate (CAS). Contrary to previous approaches that relied only on water evaporation [3], the stability of the emulsion allowed a preconcentration step by centrifugation followed by drying of the concentrated emulsion layer, and this with minute amount of stabilizer.

As hypothesized, the order of addition of the stabilizers controlled the emulsion properties via the following parameters (1) the composition of the oil-water interface, and (2) the amount and type of stabilizers (CAS, CNC) present within the continuous

phase. Moreover, the nature of the oil (hexadecane vs. olive oil) played also a significant role. Accordingly, the properties of the resulting oleogels were changed. The oleogels retained a more elastic character when prepared from starting emulsions stabilized by CNC with subsequent addition of CAS (route R3), owing to the residual free CAS present in aqueous phase. The hexadecane-based oleogel could be redispersed after drying, although the droplet sizes of these reconstituted emulsions increased. However, it was not possible to reconstitute the original emulsion for the olive oil-based oleogels.

These results demonstrate that not only the dominating species at the oil-water interface control behaviour and stability of the emulsion, but also the resulting microstructure of the oleogels after drying. A two-step emulsification process using Pickering approach in the first step followed by the introduction of a surface active protein allows the formation of very stable organogels that can be redispersed, yet containing only minute amount of stabilizer.

Multiple steps emulsification combined with a careful control of the interactions of the species at the oil-water interface constitutes a reliable approach to design soft materials fully redispersible. Based on these results, we envision that the more elastic gels can serve to encapsulate lipophilic active ingredients for release via (bio)degradation of the gel structure. On the other hand, the more viscous oleogels can be suitable for better spreading of topical ingredients on the skin.

CRedit authorship contribution statement

Lucie Urbánková: Conceptualization, Methodology, Writing - original draft. **Tomáš Sedláček:** Conceptualization, Methodology, Writing - original draft. **Věra Kašpárková:** Conceptualization, Methodology, Supervision, Writing - original draft. **Romain Bordes:** Conceptualization, Methodology, Supervision, Writing - original draft.

Declaration of Competing Interest

The authors declare that they have no known competing financial interests or personal relationships that could have appeared to influence the work reported in this paper.

Acknowledgments

This work was supported by the Czech Science Foundation (20-28732S) and by the Ministry of Education, Youth and Sports of the Czech Republic – DKRVO (RP/CPS/2020/001). LU also appreciates support of the internal grants of TBU in Zlín IGA/CPS/2019/004 funded from the resources of specific academic research. Authors would like to thank Lenka Tatarková for technical assistance.

Appendix A. Supplementary data

Supporting material contains figures S1-S7 and table T1. Supplementary data to this article can be found online at <https://doi.org/10.1016/j.jcis.2021.02.104>.

References

- [1] Y. Jiang, L. Liu, B. Wang, X. Sui, Y. Zhong, L. Zhang, Z. Mao, H. Xu, Food Hydrocoll. 77 (2018) 460, <https://doi.org/10.1016/j.foodhyd.2017.10.023>.
- [2] J. Daniel, R. Rajasekharan, J. Am. Oil Chem. Soc. 80 (2003) 417, <https://doi.org/10.1007/s11746-003-0714-0>.
- [3] A.R. Patel, P.S. Rajarethinam, N. Cludts, B. Lewille, W.H. De Vos, A. Lesaffer, K. Dewettinck, Langmuir 31 (2015) 2065, <https://doi.org/10.1021/la502829u>.
- [4] A.R. Patel, N. Cludts, M.D. Bin Sintang, A. Lesaffer, K. Dewettinck, Food Funct. 5 (2014) 2833, <https://doi.org/10.1039/c4fo00624k>.

- [5] A.I. Romoscanu, R. Mezzenga, *Langmuir* 22 (2006) 7812, <https://doi.org/10.1021/la060878p>.
- [6] H. Adelman, B.P. Binks, R. Mezzenga, *Langmuir* 28 (2012) 1694, <https://doi.org/10.1021/la204811c>.
- [7] D.C. Edmund, A.G. Marangoni, *J. Am. Oil Chem. Soc.* 89 (2012) 749, <https://doi.org/10.1007/s11746-012-2049-3>.
- [8] V. Giacintucci, C.D. Di Mattia, G. Sacchetti, F. Flammini, A.J. Gravelle, B. Baylis, J.R. Dutcher, A.G. Marangoni, P. Pittia, *Food Hydrocoll.* 84 (2018) 508, <https://doi.org/10.1016/j.foodhyd.2018.05.030>.
- [9] P. Ahmadi, M. Tabibiazar, L. Roufegarinejad, A. Babazadeh, *Int. J. Biol. Macromol.* 150 (2020) 974, <https://doi.org/10.1016/j.ijbiomac.2019.10.205>.
- [10] M.H. Naeli, J.M. Milani, J. Farmani, A. Zargaraan, *Int. J. Biol. Macromol.* 156 (2020) 792, <https://doi.org/10.1016/j.ijbiomac.2020.04.087>.
- [11] L. Alizadeh, K. Abdolmaleki, K. Nayebyzadeh, S.M. Hosseini, *J. Am. Oil Chem. Soc.* 97 (2020) 485, <https://doi.org/10.1002/aocs.12341>.
- [12] I. Capron, B. Cathala, *Biomacromolecules* 14 (2013) 291, <https://doi.org/10.1021/bm301871k>.
- [13] L. Pind'áková, V. Kašpárková, R. Bordes, *J. Colloid Interface Sci.* 557 (2019) 196, <https://doi.org/10.1016/j.jcis.2019.09.002>.
- [14] I. Capron, O.J. Rojas, R. Bordes, *Curr. Opin. Colloid Interface Sci.* 29 (2017) 83, <https://doi.org/10.1016/j.cocis.2017.04.001>.
- [15] S. Cristina Sabliov, Y. Rickey Yada, C. Hongda Chen, *Nanotechnology and Functional Foods: Effective Delivery of Bioactive Ingredients*, Wiley-Blackwell, 2015.
- [16] T.J. Wooster, M. Golding, P. Sanguansri, *Langmuir* 24 (2008) 12758, <https://doi.org/10.1021/la801685v>.
- [17] L. Bai, S. Lv, W. Xiang, S. Huan, D.J. McClements, O.J. Rojas, *Food Hydrocolloids* 96 (2019) 699, <https://doi.org/10.1016/j.foodhyd.2019.04.038>.
- [18] D.K. Sarker, M. Axelos, Y. Popineau, *Colloid Surf. B-Biointerfaces* 12 (1999) 147, [https://doi.org/10.1016/S0927-7765\(98\)00071-X](https://doi.org/10.1016/S0927-7765(98)00071-X).
- [19] V. Mikulcova, R. Bordes, V. Kasparkova, *Food Hydrocoll.* 61 (2016) 780, <https://doi.org/10.1016/j.foodhyd.2016.06.031>.
- [20] A.J. Malkin, A.I. Isayev, *Rheology: Concepts, Methods, and Applications*, ChemTec Pub, Toronto, 2017.
- [21] M. Espert, A. Salvador, T. Sanz, *Food Hydrocoll.* 109 (2020), <https://doi.org/10.1016/j.foodhyd.2020.106085>.
- [22] J.W. Goodwin, R.W. Hughes, *Rheology for Chemists*, RSC Publ, Cambridge, UK, 2008.
- [23] W. Wijaya, Q. Sun, L. Vermeir, K. Dewettinck, A.R. Patel, P. Van der Meeren, *Food Struct -Neth.* 21 (2019), <https://doi.org/10.1016/j.foostr.2019.100112>.
- [24] I. Tavernier, A.R. Patel, P. Van der Meeren, K. Dewettinck, *Food Hydrocoll.* 65 (2017) 107, <https://doi.org/10.1016/j.foodhyd.2016.11.008>.